Algorithmic aspects of enriched time domain boundary element methods

Citation for published version:
Gimperlein, H & Stark, D 2019, 'Algorithmic aspects of enriched time domain boundary element methods', *Engineering Analysis with Boundary Elements*, vol. 100, pp. 118-124.
https://doi.org/10.1016/j.enganabound.2018.02.010

Digital Object Identifier (DOI):
10.1016/j.enganabound.2018.02.010

Link:
Link to publication record in Heriot-Watt Research Portal

Document Version:
Peer reviewed version

Published In:
Engineering Analysis with Boundary Elements

Algorithmic aspects of enriched time domain boundary element methods

Heiko Gimperlein*† David Stark*

Abstract

We discuss the algorithmic aspects of a recently proposed time-domain partition-of-unity boundary element method for wave propagation problems a high frequency on coarse mesh grids. A main challenge is the accurate assembly of the Galerkin matrix for travelling plane-wave basis functions. We discuss the numerical solution of the space-time system and its preconditioning. Numerical results demonstrate the prospects and challenges of the approach.

1 Introduction

Boundary element methods provide an efficient numerical scheme for time-independent or time-harmonic scattering and emission problems. Based on an exact representation of the solution in the interior, boundary elements reduce the computation from an n-dimensional, possibly unbounded domain to its (n-1)-dimensional boundary and only require the discretisation of the boundary conditions. Recently, boundary elements have been explored for the simulation of transient phenomena, with applications e.g. to environmental noise [4] or electromagnetic scattering [33]. For the wave equation, time-dependent boundary element methods (TDBEM) were first analysed by Bamberger and Ha-Duong [2].

On the other hand, for time-harmonic wave propagation partition-of-unity, finite and boundary element methods (PUFEM / PUBEM) have emerged as a practically efficient method to achieve engineering accuracy already on very coarse meshes [26, 30, 31]. Based on plane waves as non-polynomial ansatz and test functions, the improve the difficulties with numerical pollution at high frequencies. The often allow to work on a fixed mesh, with better approximations

*Maxwell Institute for Mathematical Sciences and Department of Mathematics, Heriot–Watt University, Edinburgh, EH14 4AS, United Kingdom, email: h.gimperlein@hw.ac.uk, ds221@hw.ac.uk .

†Institut für Mathematik, Universität Paderborn, Warburger Str. 100, 33098 Paderborn, Germany

H. G. acknowledges support by ERC Advanced Grant HARG 268105 and the EPSRC Impact Acceleration Account.

obtained by increasing nuumbers of plane waves in each element. More recently, preliminary results towards time dependent finite elements with partition-of-unity enrichment in space have been obtained in [18].

To be specific, we consider transient sound radiation problems in the exterior of a scatterer Ω^-, where Ω^- is a bounded polygon with connected complement $\Omega = \mathbb{R}^3 \setminus \Omega^-$. The acoustic sound pressure field $u(t, \mathbf{x})$ due to an incident field or sources on $\Gamma = \partial\Omega$ satisfies the linear wave equation for $t \in \mathbb{R}$:

$$\begin{aligned} {c_s}^{-2}\partial_t^2 u(t,\mathbf{x}) - \Delta u(t,\mathbf{x}) &= 0 && \text{for } \mathbf{x} \in \Omega \\ u(t,\mathbf{x}) &= f(t,\mathbf{x}) && \text{for } \mathbf{x} \in \Gamma \\ u(t,\mathbf{x}) &= 0 && \text{for } t \leq 0. \end{aligned} \tag{1}$$

Here c_s denotes the wave velocity, and for simplicity we choose units in which $c_s = 1$. We make a single-layer ansatz for the solution of (1),

$$u(t,\mathbf{x}) = \int_\Gamma \frac{\phi(t-|\mathbf{x}-\mathbf{y}|,\mathbf{y})}{4\pi|\mathbf{x}-\mathbf{y}|} ds_y \qquad (\mathbf{x} \in \mathbf{\Omega}), \tag{2}$$

with $\phi = 0$ for $t \leq 0$. When $\mathbf{x}$ approaches the boundary Γ, u tends to f according to the Dirichlet boundary condition in (1). Letting $\mathbf{x}$ approach Γ on both sides of equation (2), we therefore conclude

$$f(t,\mathbf{x}) = u(t,\mathbf{x}) = \int_\Gamma \frac{\phi(t-|\mathbf{x}-\mathbf{y}|,\mathbf{y})}{4\pi|\mathbf{x}-\mathbf{y}|} ds_y =: V\phi(t,\mathbf{x}) \qquad (\mathbf{x} \in \mathbf{\Gamma}). \tag{3}$$

Equation (3) defines an equation for the single layer operator V, from which the solution of the original wave problem (1) may be recovered: If ϕ is the solution to (3), then evaluation of the integral in (2) gives the solution to (1).

This work presents the algorithmic aspects behind a recently introduced time domain partition-of-unity method for the efficient solution of time-domain boundary integral equations such as Equation (3), based on travelling plane waves as ansatz and test functions in space and time. This is the first approach to $space - timeenriched$ partition-of-unity methods, here applied to a time-dependent integral equation. It extends its counterparts for time-harmonic wave propagation to truly transient problems at higher frequencies, but still allows to work on coarse meshes. Future applications are expected in the computational acoustics of concer halls [5], the noise of inner-city traffic and high-speed trains [4].

After a short review of relevant earlier works in TDBEM and partition-of-uniy methods, we here discuss the algorithmic background of the method. We focus on the new challenges arising in time-domain with non-polynomial basis functions on coarse mesh grids. Details of the accurate quadrature to assemble the Galerkin matrix are discussed, extending the methods known for standard h-version TDBEM. We then address the efficient numerical solution of the space-time system and its preconditioning. Numerical results demonstrate key aspects of the method: Reductions of the degrees of freedom of around a factor 8, the efficient solution of the space-time system by a preconditioner, and condition numbers which are much reduced compared to partition-of-unity methods in frequency domain.

2 Background

2.1 Partition-of-unity methods

Partition-of-unity methods were first introduced and analysed by Babuska and Melenk [23, 24]. They propose the use of non-polynomial ansatz and test functions, so called enrichments, to include a priori knowledge about the behaviour of the solution into the approximation spaces. The enrichments may be used in addition to, or completely replace, the standard piecewise polynomial elements. A suitable choice of the enrichments gives rise to approximations with engineering accuracy already for low degrees of freedom and on coarse meshes. As their main drawback, the use of large numbers of basis functions in each triangle leads to ill-conditioned matrices, which poses challenges for the solution of the Galerkin equations and limits the accuracy achieved in practice for high degrees of freedom. Examples include XFEM (extended finite element method), where singular functions are included locally, for example, near a crack tip [10], and the use of plane waves in the whole domain to capture the oscillatory behaviour of solutions to time-harmonic wave problems [30, 31].

For time harmonic wave propagation and scattering, partition-of-unity boundary elements provide efficient numerical methods which are particularly suitable for large or unbounded domains. Their advantages are particularly pronounced at high frequencies, where numerical pollution increases the required computational effort for all known approaches. Seminal works in this direction include [22, 26, 27], where plane waves are added as enrichments in a standard boundary element method, with directions of propagation uniformly distributed in all directions. In a complementary direction, methods more taylored to specific geometries or based on non-standard integral formulations have been studied [7, 20].

Partition-of-unity methods have recently shown promise for transient problems, for wave [8, 18] and heat propagation [21, 25]. They are based on the existing time-independent enrichment in space and use standard time-stepping schemes to account for the time-dependence. On-going work by the authors [16] proposes a the time-dependent enrichment of space-time methods.

2.2 Time-domain boundary element methods

Boundary integral methods for the wave equation go back to Friedman and Shaw [9], resp. Cruse and Rizzo [6], their mathematical analysis to Bamberger and Ha-Duong [2]. Because the Greens function of the wave equation is concentrated on the light cone, the resulting Galerkin matrices are sparse unlike in frequency-domain, but the accurate quadrature is a main challenge. The method has been competitive for commercial applications, such as traffic and air plane noise and electromagnetic scattering, since the development of efficient MOT time stepping methods and their efficient implementation in the Ph.D. thesis of Terrasse [32]. Recent interest in boundary elements has moved towards the wave equation, with a flurry of recent progress in convolution quadrature time-stepping schemes, fast methods and adaptivity, as well as nonlinear and coupled problems [1, 3, 11, 29]. Time-domain methods are particularly relevant for the study of truly transient phenomena which are inaccessible in frequency-domain. Examples include problems in which a broad range of frequencies is involved [4, 5], or problems involving nonlinear dynamic contact and damage [12, 19].

3 Formulation

3.1 Integral formulation of the wave equation

Recall from the introduction the initial problem for the wave equation with inhomogeneous Dirichlet boundary conditions:

$$\begin{aligned} &\partial_t^2 u(t,\mathbf{x}) - \Delta u(t,\mathbf{x}) = 0 && \text{for } \mathbf{x} \in \Omega \\ &u(t,\mathbf{x}) = f(t,\mathbf{x}) && \text{for } \mathbf{x} \in \Gamma \\ &u(t,\mathbf{x}) = 0 && \text{for } t \leq 0. \end{aligned} \tag{4}$$

We make an ansatz for the sound pressure in u in terms of the single-layer potential in 3 dimensions:

$$u(t,\mathbf{x}) = \int_\Gamma \frac{\phi(t-|\mathbf{x}-\mathbf{y}|,\mathbf{y})}{4\pi|\mathbf{x}-\mathbf{y}|} ds_y \qquad (\mathbf{x} \in \boldsymbol{\Omega}) \tag{5}$$

The condition $\phi = 0$ for $t \leq 0$ represents the causal propagation of waves on the light cone. Combining (5) with the boundary condition (4), we obtain a formulation of the wave equation as an integral equation of the first kind on Γ:

$$V\phi(t,\mathbf{x}) = \int_\Gamma \frac{\phi(t-|\mathbf{x}-\mathbf{y}|,\mathbf{y})}{4\pi|\mathbf{x}-\mathbf{y}|} ds_y = f(t,\mathbf{x}) \qquad (\mathbf{x} \in \boldsymbol{\Gamma}). \tag{6}$$

The solution to the original problem (4) in a point $\mathbf{x} \in \Gamma$ is recovere from ϕ by evaluating the integral (5) in a postprocessing step.

Anisotropic space-time sobolev spaces provide the proper analytic framework for Equation (6). The space $H^s_\sigma(\mathbb{R}^+, H^r(\Gamma))$ consists of those distributions ϕ on $[0,\infty) \times \Gamma$ which vanish at $t = 0$ and whose space-time Fourier-Laplace transform $F\phi$ satisfies in local coordinates:

$$||\phi||_{s,r,\Gamma} = \left(\int\int |\omega + i\sigma|^{2s} (\omega + i\sigma)^2 + |\xi|^2)^r |F\phi(\omega + i\sigma, \xi|^2 \quad d\xi d\omega \right)^{\frac{1}{2}} < \infty \tag{7}$$

See [14, 17] for a detailed presentation.

The numerical solution of (6) is based on the following coercive weak formulation: Find ϕ such that for all ψ

$$\int_0^\infty \int_\Gamma (V\phi(t,\mathbf{x}))\partial_t\psi(t,\mathbf{x})\ ds_x\ d_\sigma t = \int_0^\infty \int_\Gamma f(t,\mathbf{x})\partial_t\psi(t,\mathbf{x})\ ds_x\ d_\sigma t\ , \tag{8}$$

with $d_\sigma t = e^{-2\sigma t}dt$. While a theoretical analysis requires $\sigma > 0$, practical computations use $\sigma = 0$ [2].

This weak formulation is well posed [17]:

Theorem 1. If $f \in H^2_\sigma(\mathbb{R}^+, H^{\frac{1}{2}}(\Gamma))$ then the retarded potential equation (7) admits a unique solution $\phi \in H^1_\sigma(\mathbb{R}^+, H^{-\frac{1}{2}}(\Gamma))$ satisfying:

$$||\phi||_{1,-\frac{1}{2},\Gamma} \leq C||f||_{2,\frac{1}{2},\Gamma} \tag{9}$$

3.2 Partition-of-unity space-time discretisation

For the solution of (8), [16] proposes a time-dependent partition-of-unity boundary element method based on numerical approximation by travelling plane waves.

To be specific, for the time discretisation we consider a decomposition of the time interval $\mathbb{R}^+$ into subintervals $[t_{n-1}, t_n]$ with constant time step Δt, such that $t = n\Delta t, \quad (n = 0, 1, 2, ..., N_t)$.

In space, we approximate Γ by a polygonal surface and denote the approximation again by Γ. We assume that $\Gamma = \cup_{i=1}^N \Gamma_i$, is a quasi-uniform triangulation, with triangular faces Γ_i. We choose a basis $\{\Lambda_1, \Lambda_2, ..., \Lambda_{N_s}\}$ of hat functions for the space of piecewise polynomials associated to the triangulation, continuous if the degree ≥ 1. Similarly, for the time discretisation we choose a basis $\{\widetilde{\Lambda}_1, \widetilde{\Lambda}_2, ..., \widetilde{\Lambda}_{N_s}\}$ of piecewise polynomial hat functions, which are continuous and vanish at $t = 0$ if the degree ≥ 1. The enrichment is best on a lattice of frequency vectors $\mathbb{K} \subset \mathbb{R}^3$.

We consider test and ansatz spaces based on tensor products of functions in space and time:

$$V_{h,\Delta t} = \text{span}\Big\{ G^i_{jl}(t,\mathbf{x}) := \widetilde{\Lambda}_i(t)\Lambda_j(\mathbf{x})\cos(\omega_i(t-t_i) - \mathbf{k}_l\cdot\mathbf{x} + \sigma_l : \\ \mathbf{k}_l \in \mathbb{K}, \omega_l = |\mathbf{k}_l|, \sigma_l \in \big\{0, \frac{\pi}{2}\big\} \Big\} \tag{10}$$

The spatial part of the enrichment corresponds to the plane waves $\cos(\mathbf{k}_l\cdot\mathbf{x}+\sigma_l)$ routinely used in partition-of-unity methods in frequency domain [26]. The spatial part has recently been used in space-enriched methods for the time domain

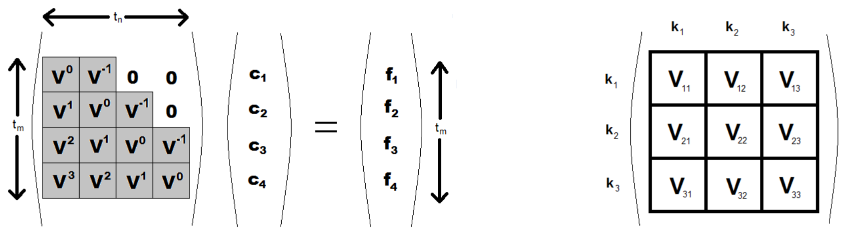

Figure 1: Full PUBEM space-time system for piecewise linear hat functions and decomposition of the blocks V^j.

[8, 18].

For $u_{\Delta t,h} \in V_{h,\Delta t}$ we thus may write

$$u_{\Delta t,h}(t, \mathbf{x}) = \sum_{i=0}^{N_t} \sum_{j=0}^{N_s} \sum_{k_i \in \mathbb{K}} c^i_{jl} G^i_{jl}(t, \mathbf{x}). \tag{11}$$

The partition-of-unity discretisation of the weak formulation (8) now reads: Find $\phi_{h,\Delta t} \in V_{h,\Delta t}$ such that for all $\psi_{h,\Delta t} \in V_{h,\Delta t}$ such that

$$\int_0^\infty \int_\Gamma (V \phi_{h,\Delta t}(t, \mathbf{x}) \partial_t \psi_{h,\Delta t}(t, \mathbf{x}) ds_x dt = \int_0^\infty \int_\Gamma f(t, \mathbf{x}) \partial_t \psi_{h,\Delta t}(t, \mathbf{x}) ds_x dt \tag{12}$$

From the solution $\phi_{h,\Delta t}$, the numerical approximations $u_{h,\Delta t}$ to the solution of the wave equation (4) is obtained in Ω by evaluating the integral of the single-layer potential in (5) numerically.

As a conforming Galerkin discretisation, Equation 8 admits a unique solution and leads to a stable partition-of-unity method in space-time.

3.3 Quadrature method for retarded potentials

A main challenge of the PUBEM (8) is the accurate and efficient assembly of the Galerkin matrix. As depicted in Figure 1, the matrix is a block Toeplitz matrix where every block corresponds to a time step. Each of the blocks decomposes into blocks for the individual enrichments $\mathbf{k}_i$. Because of causality the spacetime matrix is almost lower triangular: If the hat functions in time are piecewise polynomials of degree q, blocks which are more than q bands above the diagonal vanish.

The blocks of the matrix are explicitly given by

$$V^i = \int_0^\infty \int_{E(T) \cap \hat{T}} \int_{E(\mathbf{x}) \cap T} \frac{G^m_{jl}(t - |\mathbf{x} - \mathbf{y}|)}{4\pi |\mathbf{x} - \mathbf{y}|} \partial_t G^{m+i}_{j'l'}(t, \mathbf{x}) \quad ds_y ds_x dt \tag{13}$$

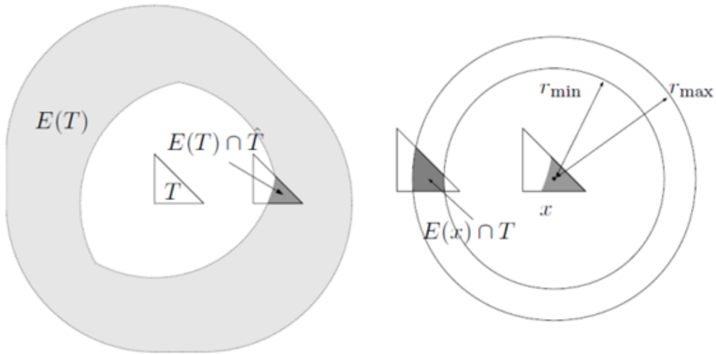

Figure 2: Outer (left) and inner (right) integration.

Here T and $\hat{T}$ are the test and trial elements. $E(\mathbf{x})$ the light cone around $\mathbf{x}$ and $E(T)$ the union of light cones around points in T. See Figure (2). $i \in \{1, 2, ..., N_t\}$ indexes the time nodes. After an analytical evaluation of the time integral, the inner ($\mathbf{y}$) integral requires integration over geometrically complicated intersections of triangles with lightcone shells, with a singular integrand $|\mathbf{x} - \mathbf{y}|^{-1}$:

$$V^i = \int_0^\infty \int_{E(T)\cap\hat{T}} \int_{E(\mathbf{x})\cap T} \frac{1}{|\mathbf{x} - \mathbf{y}|} \Lambda_j(\mathbf{y})\Lambda_{j'}(\mathbf{x}) F(\mathbf{y}, \mathbf{x}, \mathbf{k}_l, \omega_l, \mathbf{k}_{l'}, \omega_{l'}) \quad (14)$$

for an explicitly given function F, given below in Section 4.1.

Difficulties arise: Kernel singularities when $|\mathbf{x} - \mathbf{y}|$ approaches zero, geometric singularities in F at the boundary of light cones (see below), and the oscillatory behaviour of the basis functions for large $\mathbf{k}_l$, $\mathbf{k}_{l'}$. The first problem is standard in BEM, and we avoid it by using a quadrature hp-graded towards the singularity at $|\mathbf{x} - \mathbf{y}| = 0$.

More precisely, the following graded quadrature is performed to evaluate an integral of the form $\int_0^b f\,ds$ in the normal direction to $s = |\mathbf{x}-\mathbf{y}| = 0$. Denote by $Q_n^{[0,b]} f := \sum_{i=1}^n w_i f(x_i)$ the Gauß-Legendre quadrature rule with n quadrature points. Given a subdivision of $[0, b]$ into m subintervals I_j, define a composite Gauß rule with degree vector $\mathbf{n} = (n_1, \dots, n_m)$ by $Q_{n,m,\sigma} f := \sum_{j=1}^m Q_{n_j}^{I_j} f$. We use a geometric subdivision of $[0, b]$ with m levels and grading parameter $\sigma \in (0, 1)$: $[0, b] = \bigcup_{j=1}^m I_j$, where for $j = 1, \dots, m$ we let $I_j := [x_{j-1}, x_j]$, $x_0 := 0$, $x_j := b\sigma^{m-j}$ with suitable $\mathbf{n}$. See [28] for an analysis of this quadrature for time-independent integral equations.

For the second problem, we project the point of observation $\mathbf{x}$ onto the triangle plane and use a careful decomposition of the area of integration into smple

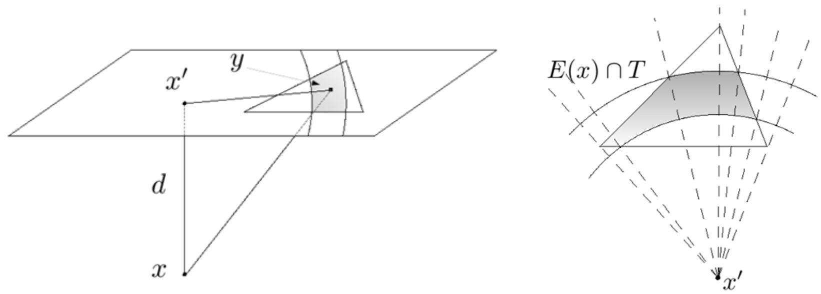

Figure 3: Projection of point of observation ($\mathbf{x}$) onto the triangle plane (left). Partitioning of the area of integration for inner quadrature (right).

standard shapes D_i in polar coordinates. The inner integral thus becomes:

$$\sum_{l=1}^{n_d} \int_{D_l} |d^2 + r^2|^{\frac{p-1}{2}} \Lambda(\mathbf{y}) ds_y \tag{15}$$

To evaluate the integrals over D_i, we apply seperate graded quadratures in the radial and angular variables, with at least 10 Gauss points per wave length to resolve oscillations. See Figure 3.

The outer integral is less singular and ses a standard composite Gauss quadrature with at least 10 points per wavelength.

3.4 Detailed analysis of integration in F

A more detailed analysis shows that the matrix entries are of the form:

$$= \int_0^\infty \int_\Gamma \int_\Gamma \frac{1}{|\mathbf{x}-\mathbf{y}|} \widetilde{\Lambda}_m(t-|\mathbf{x}-\mathbf{y}|) \Lambda_m(\mathbf{y}) \cos\Big(\omega_m(t-t_m-|\mathbf{x}-\mathbf{y}|)-\mathbf{k}_m\cdot\mathbf{y}+\sigma_m\Big)\, ds_y$$

$$\cdot \quad \Big[\dot{\widetilde{\Lambda}}_n(t)\Lambda_n(\mathbf{x}) \cos\Big(\omega_n(t-t_n)-\mathbf{k}_n\cdot\mathbf{x}+\sigma_n\Big) - \widetilde{\Lambda}_n(t)\Lambda_n(\mathbf{x}) \sin\Big(\omega_n(t-t_n)-\mathbf{k}_n\cdot\mathbf{x}+\sigma_n\Big)\omega_n\Big]\, ds_x dt. \tag{16}$$

The hat functions $\widetilde{\Lambda}_m$ and $\widetilde{\Lambda}_n$ exhibit four nontrivial cases of overlap, see Figure 4. The resulting kinks in F are exhibited in Figure 5.

3.5 A preconditioner for PUBEM

The space-time systems as in Figure 1, which arise from standard polynomial h-method time domain Galerkin boundary element discretisations with piecewise

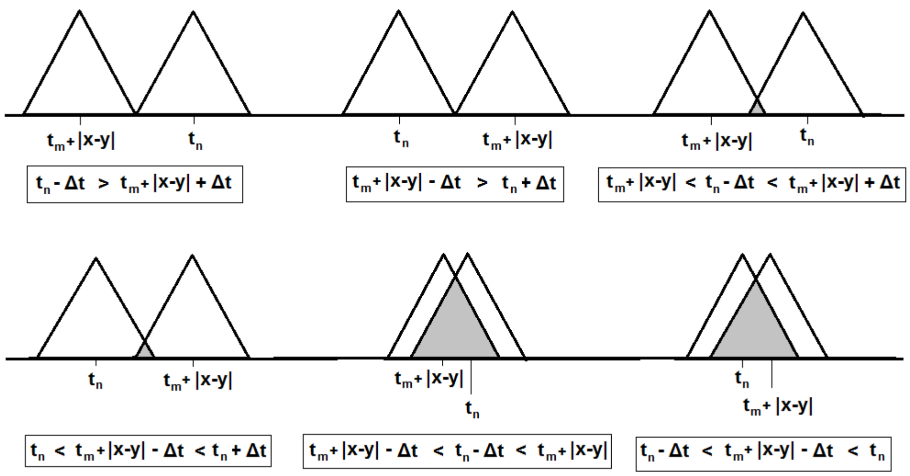

Figure 4: Possible intersections of temporal basis functions.

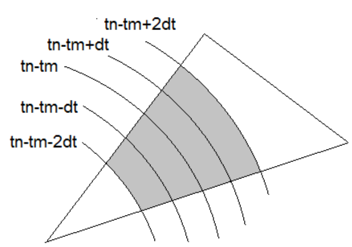

Figure 5: Division ino light cones corresponding to cases in Figure 4.

constant test functions hat functions $\widetilde{\Lambda}_n(t)$ in time, are lower triangular. Indeed, for a matrix block

$$V^i = \int_0^\infty \int_{E(T)\cap\hat{T}} \int_{E(\mathbf{x})\cap T} \frac{\widetilde{\Lambda}_m(t-|\mathbf{x}-\mathbf{y}|)}{4\pi|\mathbf{x}-\mathbf{y}|} \partial_t \widetilde{\Lambda}_{m+i}(t,\mathbf{x}) \quad ds_y ds_x dt \tag{17}$$

with piecewise constant test functions $\widetilde{\Lambda}_{m+i}$, the argument $t-|\mathbf{x}-\mathbf{y}|$ of the ansatz function lets the integrand vanish whenever $i<0$. In particular, the block V^{-1} in Figure 1 is 0. The resulting space-time system may then be solved by backsubstitution, which leads to efficient time stepping schemes.

For test functions of order q, the space-time systems has q bands of blocks above the diagonal. Nevertheless, an extrapolation leads to efficient time stepping schemes with engineering accuracy, as is adequate for the use in partition-of-unity methods. We discuss the approach for piecewise linear functions.

Denoting the solution vector at time t_{j+1} by c^{j+1}, one approximates its value from previous time steps by extrapolation $c^{j+1} \approx c^j + (c^j - c^{j-1})$ in order to eliminate the blocks V^i for $i<0$ in Figure 1. For smooth solutions the error of this approximation is of the order of the time step Δt, and therefore of a similar size as the error from the finite element approximation. Substituting this value $c^{j+1} \approx c^j + (c^j - c^{j-1})$ into the space-time systems:

$$F^j = V^1 c^{j-1} + V^0 c^j + V^{-1} c^{j+1} \approx (V^1 - V^{-1}) c^{j-1} + (V^0 + 2V^{-1}) c^j. \tag{18}$$

The result is a block Toeplitz equation $\widetilde{V}c = F$ in space-time, which is block lower triangular in the sense that $\widetilde{V}^i = 0$ for $i<0$. This system can now be stably solved by backsubstitution. Here the bands are given by

$$\widetilde{V}^0 = (V^0 + 2V^{-1}), \widetilde{V}^1 = (V^1 - V^{-1}), \widetilde{V}^j = V^j \quad \text{if} \quad j > 1. \tag{19}$$

The resulting time-stepping scheme may be used either as a stand-alone solver or as a preconditioner for GMRES applied to the space-time matrix. Both have been studied in a variety of wave propagation and scattering problems in [15]. In the current paper we employ (18) as a preconditioner of the PUBEM.

Instead of preconditioned GMRES, one may use special solvers for Toeplitz systems. However, the preconditioner suffices for all applications considered so far, and special solvers for non-symmetric block Toeplitz systems do not seem to be readily available in standard libraries.

4 Numerical experiments

Example 1 : For a regular icosahedron Γ, Figure 6, of diameter 2 and centered in $(0,0,0)$, we use the right hand side $f(t,\mathbf{x}) = \exp(-25/t^2)\cos(\omega_f t - \mathbf{k}_f \mathbf{x})$. f represents a plane wave with $\mathbf{k}_f = (1.5, 3, 8.5)$ which is smoothly turned on for times $[0,5]$. The partition-of-unity TDBEM approximation from (12) is compared to an h-method TDBEM with piecewise linear ansatz and test functions on a uniform mesh with up to 1280 triangles and constant CFL ratio $\frac{\Delta t}{\Delta x} = 0.19$. Figure 6 depicts the h-method solution ϕ at times 3.8, 4.2 and 4.6 and the fine mesh of 1280 triangles used for its computation.

Figure 7a illustrates the solution of the partition-of-unity method, evaluated in the centroid $(0.46, 0.46, 0.46)$ of a triangle. The partition-of-unity TDBEM uses a mesh of 20 triangles as in the left-most picture in Figure 6 and n enrichment functions in each triangle, for $n \leq 15$ and $\Delta t = 0.1$, resp. 0.2.

For a variational method as discussed in this paper, a natural measure of the error is the energy defined by the single layer operator, which is computed from the stiffness matrix V, the right hand side vector f and the solution vector c as $E(c) = \frac{1}{2}c^\top V c - c^\top f$. We compute the relative energy error with respect to the energy E_∞ of an extrapolated benchmark energy as $\frac{E(c)-E_\infty}{E_\infty}$. This energy error is is relevant also because it controls the resulting pointwise error of the sound pressure u to the original problem (1), as obtained from ϕ by evaluating the integral (2).

Figure 7b compares the convergence of the relative energy error between the above-described h-method and the partition-of-unity method as the total number of space-time degrees of freedom is increased. While the h-method shows a well-known linear convergence [13], the partition-of-unity method exhibits its typical nonlinear convergence with abrupt decreases. The precise errors are detailed in Table 1. The partition-of-unity method here reduces the space-time degrees of freedom by a factor up to 8, indicating the potential of the method. The savings in the degrees of freedom translate into reduced computation times also in the time-domain, see [8, 21].

Example 2 : We consider the preconditioner for plane wave scattering problems in different geometries. With the same right hand side, ansatz and test functions as in Example 1, we study the numerical solution of (12) on the screen $\Gamma = [0,1]^2 \times \{z = 0\}$ as well as on the regular icosahedron from Example 1. The time step used is $\Delta t = 0.1$ for the partition-of-unity method.

The space-time equation (12) for the partition-of-unity TDBEM is solved with GMRES and a preconditioned GMRES, with the preconditioner from Section 3.5 as the number of enrichment functions is increased. We compare the results to those obtained for the h-method TDBEM with piecewise linear ansatz and test functions on a uniform mesh, with GMRES, resp. the preconditioned GMRES of Section 3.5. We use the meshes and the time step as in Example 1.

For the icosahedron Figure 8a shows number of GMRES iterations required to reduce the norm of the residual $\|Vc - f\|$ below 10^{-9}. They are plotted against the number of space-time degrees of freedom, as the number of enrichments is increased for the partition-of-unity method, respectively as the mesh size is decreased for the h-method. The precise iteration numbers for the partition-of-unity method are collected in Table 2. For both methods the pre-

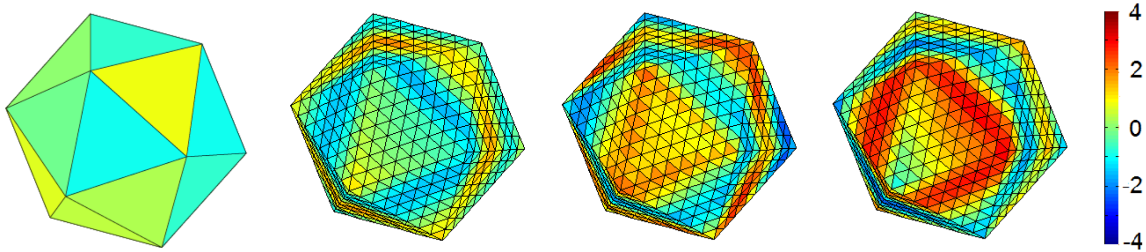

Figure 6: Example 1 - meshes for PU (20 triangles) and h-method (1280 triangles), density at $t = 3.8, 4.2, 4.6$.

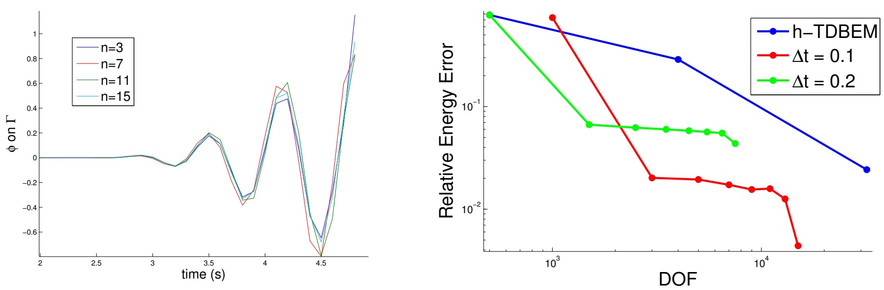

Figure 7: Example 1 - a) density ϕ at point $(0.46, 0.46, 0.46)$, b) relative error in energy: h-method, PU with $\Delta t = 0.1, 0.2$.

conditioner leads to a significant reduction of the number of iterations. Because the preconditioner is based on linear extrapolation in time and the time step Δt goes to 0 in the h-method, the number of preconditioned GMRES iterations is stable in this case. For the partition-of-unity method, Δt is fixed but a practically significant reduction is nevertheless observed.

Figure 8b shows condition number of the matrix relating to each geometry considered, for a range of space-time degrees of freedom. The condition numbers easily reach 10^{16} for partition-of-unity methods in frequency domain, the additional time dimension here limits the condition numbers to around 10^7.

n	DOF	error PU ($\Delta t = 0.2$)	DOF	error PU ($\Delta t = 0.1$)	DOF	rel. error h
1	500	0.78	1000	0.76	500	0.78
3	1500	0.065	3000	0.020	4000	0.28
5	2500	0.063	5000	0.019	20000	0.025
7	3500	0.060	7000	0.017		
9	4500	0.058	9000	0.0145		
11	5500	0.057	11000	0.015		
13	6500	0.055	13000	0.012		
15	7500	0.0042	15000	0.0043		

Table 1: Errors of the PU and h-methods corresponding to Figure 7b.

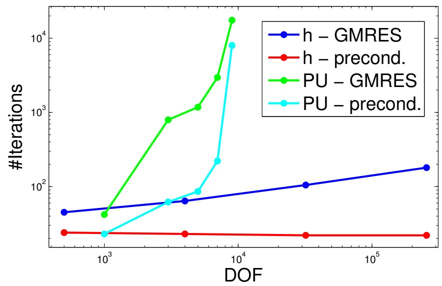

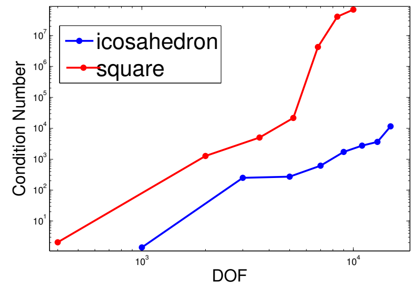

Figure 8: a) GMRES vs. preconditioned GMRES, b) condition number of $\mathbf{V}^0$ for PU.

n	DOF	iter. PU - GMRES	iter. precond
1	1000	41	24
3	3000	795	62
5	5000	1.15×10^3	87
7	7000	3.0×10^3	2.1×10^2
9	9000	1.8×10^4	8.1×10^3

Table 2: Necessary GMRES iterations corresponding to Figure 8a.

References

[1] T. Abboud, P. Joly, J. Rodriguez, I. Terrasse. Coupling discontinuous Galerkin methods and retarded potentials for transient wave propagation on unbounded domains. Journal of Computational Physics, 230 (2011), 5877-5907

[2] A. Bamberger, T. Ha Duong, Formulation variationnelle espace-temps pour le calcul par potentiel retard de la diffraction d'une onde acoustique. Math. Methods in the Appl. Sciences 8 (1986); 405-435 and 598-608.

[3] L. Banjai, M. Schanz. Wave propagation problems treated with convolution quadrature and BEM. Lecture Notes Applied Computational Mechanics 63, Fast boundary element methods in engineering and industrial applications, pp. 145-184. Springer, (2012).

[4] L. Banz, H. Gimperlein, Z. Nezhi, E. P. Stephan. Time domain BEM for sound radiation of tires. Computational Mechanics 58 (2016), 45-57.

[5] J. Chabassier, A. Chaigne, P. Joly. Modeling and simulation of a grand piano. J. Acoustical Society of America, vol. 1 (2013), 666-685.

[6] T. A. Cruse, F. J. Rizzo. A direct formulation and numerical solution of the general transient elastodynamic problem, I. J. Math. Analysis Appl. 22 (1968), 244-259.

[7] S. N. Chandler-Wilde, I. G. Graham, S. Langdon, E. A. Spence. Numerical-asymptotic boundary integral methods in high-frequency acoustic scattering. Acta Numerica 21 (2012), 89-305.

[8] M. Drolia, M. S. Mohamed, O. Laghrouche, M. Seaid, J. Trevelyan. Enriched finite elements for initial-value problem of transverse electromagnetic waves in time domain. Computers and Structures 182 (2017), 354-367

[9] M. Friedmann, R. Shaw. Diffraction of pulses by cylindrical obstacles of arbitrary cross section, Journal of Applied Mechanics 29 (1962), 40-46.

[10] T. P. Fries, T. Belytschko. The extended/generalised finite element method: An overview of the method and its applications. International Journal for Numerical Models in Engineering 84 (2010), 253-304.

[11] H. Gimperlein, M. Maischak, E. P. Stephan. Adaptive time domain boundary element methods and engineering applications. Journal of Integral Equations and Applications 29 (2017), 75-105.

[12] H. Gimperlein, F. Meyer, C. Oezdemir, E. P. Stephan. Time domain boundary elements for dynamic contact problems, preprint.

[13] H. Gimperlein, F. Meyer, C. Oezdemir, D. Stark, E. P. Stephan. Boundary elements with mesh refinements for the wave equation, to appear in Numer. Math. (2018).

[14] H. Gimperlein, Z. Nezhi, E. P. Stephan. A priori error estimates for a time-dependent boundary element method for the acoustic wave equation in a half-space, Math. Methods in the Appl. Sciences 40 (2017), 448-462.

[15] H. Gimperlein, D. Stark. Extrapolation as precondition for time domain boundary element methods, preprint.

[16] H. Gimperlein, D. Stark. A partition-of-unity boundary element method for transient wave propagation, preprint.

[17] T. Ha Duong. On retarded potential boundary integral equations and their discretisations. Topics in computational wave propagation, Lect. Notes Comput. Sci. Eng., Vol. 31. Springer: Berlin, 301-336.

[18] S. Ham, K.J. Bathe. A Finite Element Method Enriched For Wave Propagation Problems. Computers and Structures 94-95 (2012), 1-12.

[19] G. D. Hatzigeorgiou, D. E. Beskos. Dynamic inelastic structural analysis by the BEM: A review. Engineering Analysis with Boundary Elements 35 (2011),159-169.

[20] D. P. Hewett, S. Langdon, N. Chandler-Wilde. A Frequency-independent Boundary Element Method for Scattering by Two-Dimensional Screens and Apertures. IMA Journal of Numerical Analysis 35 (2015), 1698-1728.

[21] M. Iqbal, H. Gimperlein, M. S. Mohamed, O. Laghrouche. An a posteriori error estimate for the generalised finite element method for transient heat diffusion problems. International Journal for Numerical Methods In Engineering 110 (2017), 1103-1118.

[22] O. Laghrouche, P. Bettess, E. Perrey-Debain, J. Trevelyan. Wave interpolation fine elements for Helmholtz problems with jumps in the wave speed. Computer Methods in Applied Mechanics and Engineering, 194 (2005), 367-381.

[23] J. M. Melenk, I. Babuska. The partition of unity finite element method: Basic theory and applications. Computer Methods in Applied Mechanics and Engineering, 139 (1996), 289-314.

[24] J. M. Melenk, I. Babuska. The partition of unity method. International Journal for Numerical Methods in Engineering, 40 (1997), 727-758.

[25] M. S. Mohamed, M. Seaid, J. Trevelyan, O. Laghrouche. A partition of unity FEM for time-dependent diffusion problems using multiple enrichment functions. International Journal for Numerical Methods in Engineering 93 (2013), 245-265.

[26] E. Perrey-Debain, J. Trevelyan, P. Bettess. Wave boundary elements: A theoretical overview presenting applications in scattering of short waves. Engineering Analysis with Boundary Elements 28 (2004), 131-141.

[27] E. Perrey-Debain, J. Trevelyan, P. Bettess. On Wave Boundary Elements for Radiation and Scattering Problems with Piecewise Constant Impedance. IEEE Transactions on Antennas and Propagation 53 (2005), 876-879.

[28] C. Schwab, *Variable order composite quadrature of singular and nearly singular integrals*, Computing 53 (1994), 173-194.

[29] F. J. Sayas. Retarded potentials and time domain boundary integral equations: a road-map. Springer Series in Comp. Math. 50, Springer (2016).

[30] T. Strouboulis, I. Babuska, R. Hidajat. The generalized finite element method for Helmholtz equation: Theory, computation, and open problems. Computer Methods in Applied Mechanics and Engineering, 195 (2006), 4711-4731.

[31] T. Strouboulis, R. Hidajat, I. Babuska. The generalized finite element method for Helmholtz equation part ii: Effect of choice on handbook functions, error due to absorbing boundary conditions and its assessment. Computer Methods in Applied Mechanics and Engineering, 197 (2008), 364-380.

[32] I. Terrasse. Resolution mathematique et numerique des equations de Maxwell instationnairs par une methode de potentiels retardes. Ph.D. thesis, Ecole Polytechnique (1993).

[33] A.E. Yilmaz, J.-M. Jin, E. Michielssen. Time domain adaptive integral method for surface integral equations. IEEE Transactions on Antennas and Propagation 52 (2004), 2692-2708.